Crystals **2012**, *2*, 1261-1282; doi:10.3390/cryst2031261

OPEN ACCESS

crystals

ISSN 2073-4352

www.mdpi.com/journal/crystals

Review

Electronic Principles of Hydrogen Incorporation and Dynamics in Metal Hydrides

Nenad Ivanović, Nikola Novaković, Ivana Radisavljević, Ljiljana Matović and Jasmina Grbović Novaković *

Vinča Institute of Nuclear Sciences, University of Belgrade, 11001 Belgrade, Serbia;
E-Mails: nivanov@vinca.rs (N.I.); novnik@vinca.rs (N.N.); iva@vinca.rs (I.R.);
ljiljam@vinca.rs (L.M.)

* Author to whom correspondence should be addressed; E-Mail: jasnag@vinca.rs;
Tel.: +381-11-3408-552; Fax: +381-11-3408-224.

Received: 20 March 2012; in revised form: 14 July 2012 / Accepted: 18 July 2012 / Published: 30 August 2012

Abstract: An approach to various metal hydrides based on electronic principles is presented. The effective medium theory (EMT) is used to illustrate fundamental aspects of metal-hydrogen interaction and clarify the most important processes taking place during the interaction. The elaboration is extended using the numerous existing results of experiment and calculations, as well as using some new material. In particular, the absorption/desorption of H in the Mg/MgH_2 system is analyzed in detail, and all relevant initial structures and processes explained. Reasons for the high stability and slow sorption in this system are noted, and possible solutions proposed. The role of the transition-metal impurities in MgH_2 is briefly discussed, and some interesting phenomena, observed in complex intermetallic compounds, are mentioned. The principle mechanism governing the Li-amide/imide transformation is also discussed. Latterly, some perspectives for the metal-hydrides investigation from the electronic point of view are elucidated.

Keywords: hydrogen storage; metal hydrides; MgH_2; complex hydrides; Li-amide/imide; electronic structure; *ab initio* calculation; DFT; sorption kinetics; catalysts

---

1. Introduction

Metal hydrides represent promising technology for cleaner, cheaper and more efficient energy production [1–14]. They are also systems of considerable theoretical interest [15–25] convenient for investigation of fundamental interactions that are expected to be important in new complex materials [26–32]. Although significant experimental and theoretical work has been devoted to the study of metal hydrides, some of their fundamental features, such as details of valence and conduction bands and energy gap structures, the charge transfer and the charge distribution, the origin and the importance of various contributions to the bonding between metal and hydrogen (M–H) and hydrogen and hydrogen (H–H), are not yet fully clarified. A complete elaboration of these topics from the first principles is indispensable for understanding of H-behavior in metallic systems in general. Moreover, extensive data about metal hydrides have been obtained and explained using various, and sometimes contradictory, concepts [15–18,20–26,33–39]. However, a coherent approach valid for all metal hydrides is still missing. To better illustrate these points, we will focus attention on one of the most investigated M–H systems, MgH_2, and extend the elaboration with some instructive and interesting examples found for other metal hydrides.

Due to its high hydrogen capacity by weight (7.6 wt.%) and its low cost, MgH_2 is considered to be a promising candidate for hydrogen storage applications. However, several disadvantages, like the high temperature of sorption, plateau pressure of 1 bar at 552 K, and slow sorption kinetics, prevent its practical use [1,2,40]. To overcome these drawbacks, it is necessary to understand the nature of bonding and mechanisms that govern hydrogen behavior in magnesium-based hydrides. Even though detailed experimental and theoretical [3–8,34,40–52] studies have been performed on these tasks, sorption kinetics has not yet been understood, since the Mg–H interaction is strongly influenced by the synthesis method and the presence of additives. For instance, ball milling [3–8,42,43] causes mechanical deformation, surface modification, and metastable phase formation, and generally promotes the solid-gas reaction: defect zones may accelerate the diffusion of hydrogen, and defect clusters may lower the barrier for nucleation of MgH_2. Addition of metals [53,54], transition metals [3,4,6–8,41,44,55–62], metal oxides [61–63], or intermetallic compounds [62,64] as catalysts to mechanically milled MgH_2, usually decreases its thermal stability and decomposition temperature and enhances sorption kinetics. Since nanosized powders are specific systems with properties controlled by their dimensions, they have been recognized as a possible solution for the problem of hydrogen sorption kinetics [7,10]. However, dealing with nanomaterials has its difficulties regarding exact characterization [45]. Obviously, it is important to correlate the specific type of defects, their concentration and distribution in MgH_2, and induced changes of H-dynamics and sorption properties. One attempt was to improve the sorption properties by heavy ions [45,46] and ultrasonic irradiation [52].

However, the electronic aspects of these numerous and versatile phenomena induced in MgH_2 by various treatments have not yet been completely resolved, even though a large number of theoretical and computational investigations [42,44,48–51,65–72] have been reported. In one such early report, the Born-Mayer type of calculations of the MgH_2 lattice energy was performed, assuming that the compound was purely ionic [19]. The obtained cohesion was larger than experimentally observed which is an indication of the covalent bonding contribution to MgH_2 [49]. Although each of the

aforementioned calculations [42,44,48–51,65–72] give some information, a complete and coherent explanation of numerous experimental findings has not been found.

In this paper we have made an attempt to elaborate a general and straightforward procedure for understanding the most important processes appearing during the metal-hydrogen interaction, at a fundamental, electronic level. For that purpose we extended our previous experimental [33,44,45], and known numerical [20,23,32,44,65] results by first-principle calculations of the electronic structures of various metal hydrides using the Full Potential Augmented Plane Waves extended (FP-APW+lo) and the Full Potential Linearized Augmented Plane Waves (FP-LAPW+LO) with addition of local orbitals methods, as implemented in the WIEN2k software package [73], and the pseudopotentials method, as implemented in Abinit software package.

Along with our results we have provided a concise overview of the existing experimental and theoretical knowledge that, we believe, supports the subject matter of this paper in the most appropriate manner. We insist more on a clear and consistent approach, than on details of a huge amount of experimental and theoretical data existing for metal hydrides.

2. Results and Discussion

2.1. The Basic Features of the Metal-Hydrogen Interaction

It is instructive to start considerations of metal–hydrogen (M–H) interaction using concepts simple enough to afford a clear physical picture, but at the same time accurate enough to provide results of significant interest. Such a starting point could be the Effective Medium Theory (EMT) [74]. The basic idea of EMT is to replace, in the first approximation, the energy change of an atom (molecule, cluster) interacting with an inhomogenous host, with the energy change ΔE_{hom} valid if it is embedded in a homogenous electron gas of density ρ_o equal to the density of the host ρ_h at the embedding position. Then, if necessary, corrections accounting for the specific features of the ρ_h, embedding system characteristics, and their interaction should be introduced. This approach offers numerous advantages:

- $\Delta E_{\text{hom}}(\rho)$ can be calculated for a particular atom (molecule, cluster) and tabulated, which has been done for numerous atoms [75,76].
- The mentioned corrections of the host and the embedding system due to various perturbations including their interaction can, in most cases, be obtained by a rather simple procedure [74,75,77].
- The EMT is based on the Density Functional Theory (DFT), so its results could be easily related to the results of the state-of-art computations, especially in Local Density Approximation (LDA), although the relations to other approximations for exchange-correlation interaction have been made [75].

However, most important of all, the approach offers a clear insight into various physical processes taking place during the host-embedding system (in our case M–H) interaction at the electronic level. This particular insight is not always obvious from the results of extensive first-principle calculations. To illustrate this point, we will mention here the most interesting general results that model has provided for the M–H interaction, as well as some specific results for the particular aspect of this interaction, which will be elaborated in more detail in the chapters that follow.

Figure 1. Principle sketch of the energy change of H atom embedded in the homogenous electron gas of various densities, $\Delta E_{hom}(\rho)$, and the corresponding cohesion energy $\Delta E_{coh}(\rho)$, obtained by appropriate corrections [75].

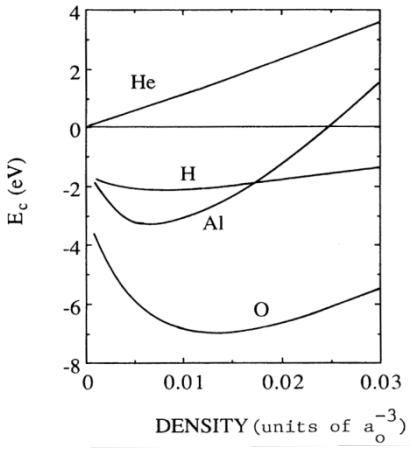

1. The most significant contribution to $\Delta E_{coh}(\rho)$ comes from the tendency of H to form a negative ion, so the models based on covalency or similar concepts are inappropriate for the description of M–H interaction.
2. As the electron affinity of H (A_H) is smaller than the metal work function (φ_M), H goes to the neutral atom limit far from the metal surface (if H–H→H_2 recombination does not take place)
3. The minimum of $\Delta E_{hom}(\rho)$ for H is placed in the ρ range between 0.002 a.u. [74], 0.0055 a.u. [75] and 0.012 a.u. [70], so one can expect that H will prefer to occupy the positions with electron densities in that range, or as close as possible to it. This means that H_2 may approach the more open and low electron density metallic surfaces closer (in general bcc closer than fcc [74], in particular the hypothetic (100) of the fcc Mg closer than the (0001) of the hcp Mg [77]), and experience smaller adsorption barriers. For instance the adsorption barrier for H on Al surface is deeper and more distant from the surface than for Mg, and it almost vanishes for low electron density Na surface [74].

The $\Delta E_{hom}(\rho)$ dependence also predicts that H will prefer the most open structures inside the metals, e.g., octahedral interstices in fcc and hcp, and tetrahedral interstices in bcc structures, and that higher diffusion barriers could be more relevant in fcc or hcp than in bcc metals, due to the larger ρ at the saddle point in the denser structures [78]. For the same reasons, H will be instable in the high electron density bulk of Al, and be of about the same stability in the Mg bulk as on its surface, and much more stable in the bulk than on the surface of Na, explaining the low solubility of H in Al, and the quite different behavior of H in Mg and Na.

Obviously, the EMT offers a quite general and transparent picture of processes during the M–H interaction, predicting the H (and H_2) behavior close to, and on the particular metallic surface, as well as in the bulk. In the following sections we will consider these processes in more detail using also the results of more accurate calculations and experiment.

2.2. H_2 Adsorption and Dissociation of H_2 on Mg (0001) Surface

One large success of EMT, was the explanation of H_2 adsorption and dissociation on the hcp Mg (0001) surface [77]. To illustrate this, charge distribution on the Mg (0001) surface calculated by the pseudopotentials method as implemented in the Abinit package [79] is presented in Figure 2. The results of EMT can be briefly presented as follows:

- There is an activation barrier for H_2 adsorption on the Mg (0001) surface, which directs it toward the atom (A) (above the Mg atom) position, where H_2 is placed parallel to the surface. The adsorption barrier arises because the H_2 interaction with the surface charge starts to weaken the H–H bond before H–Mg bonding appears. This produces the first "delay" in the H absorption kinetics on the Mg (0001) surface.
- Dissociation of H_2 at the (A) position is hindered with another activation barrier (of about 0.5 eV), but H_2 is almost free to move above the surface toward the bridge (B) site above the line connecting two neighboring surface Mg atoms. This produces the second "delay" in the H absorption kinetics on the Mg (0001) surface.
- Dissociation barrier at the (B) position is quite low (about 0.1 eV, producing the third "delay" in the H absorption kinetics on the Mg (0001) surface), and after dissociation, one H atom goes into the surface C_{fcc} site, and the other into the surface C_{hcp} site, and then quickly move into the first neighboring unoccupied C_{fcc} site (producing the fourth "delay" in the H absorption kinetics on the Mg (0001) surface), which is energetically most favorable for H adsorption. These C_{fcc} sites are the starting positions for H diffusion into the bulk of Mg metal.

Figure 2. The charge distribution on the Mg (0001) surface calculated using the pseudopotentials method (Abinit). The characteristic positions on the surface are denoted: atop-(A), bridge-(B), Center fcc-(C_{fcc}) and hcp-(C_{hcp}).

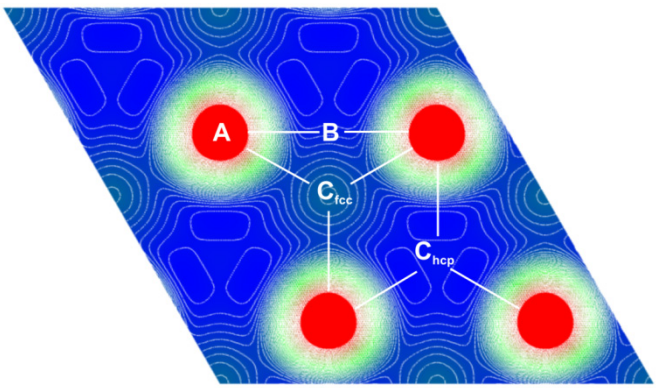

It has been established [77] that dissociation of H_2 depends on the filling of its antibonding resonant state, and this filling depends on the nature and amount of the surface electron density, and its extension above the surface, explaining quite simply the above mentioned positioning of H_2 (and H) and their behavior on the Mg (0001), and generally, any other surface.

The results of more accurate calculations [67,79,80] and experiments [81,82] support the presented picture, even though some values are a bit different. For instance, distance of H_2 dissociation (also at (B) position) from the Mg (0001) surface was obtained in [67] to be d_{dis} = 1.02 Å, and the

dissociation barrier E_{dis} = 1.05 eV, is in good agreement with experiment [81]. The analyses of the results have shown that a major discrepancy arises from the LDA approximation of the exchange-correlation potential used in EMT, and some control calculations in [67]. The calculations also confirm the C_{fcc} positions as the final state for the H adsorption on the Mg (0001) surface.

2.3. H Diffusion into the Bulk of Mg, and Hydrides Phase Formation

After dissociation of H_2 and accommodation of H at the most convenient surface positions, H diffuses into the bulk of Mg metal. The EMT predicts that H is going to search for the positions inside the hcp structure of Mg with the most appropriate ρ value, which are the octahedral interstices.

Figure 3. Crystal structure of hcp-Mg with octahedral and tetrahedral interstitial cites denoted. Wurtzite structure is a hcp derived structure with only half the (T+ or T−) tetragonal sites populated. Similarly, CdI_2 differs from NiAs structure having only half of the octahedral sites populated.

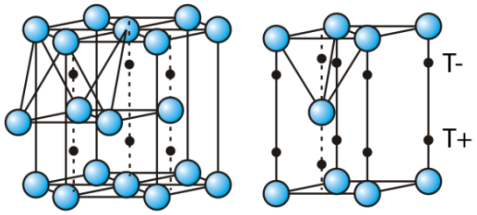

As the H concentration increases during hydrogenation, it is very important to establish positions of its further incorporation into the Mg crystal lattice. This pattern of H-accommodation into the Mg lattice, which influences the kinetics of H absorption and probability for various hydride phases formation was the subject of several investigations [37,50,65,66]. *Ab initio* calculations of Schimmel *et al.* [50] suggest that hydrogen diffuses through the Mg metal phase, jumping between octahedral and/or tetrahedral interstitials, and that for large Mg particles and low temperatures, hydrogen diffusion is not expected to be the limiting factor of H kinetics. According to our investigations [65], the H incorporation into the Mg crystal lattice proceeds as follows:

After H has populated the first sub-surface row of octahedral interstices, it diffuses toward, not the first, but the next neighbouring row of octahedral interstices in an attempt to form an ordered Mg_2H structure of the CdI_2 structure type (Figure 4a), which is, although thermodynamically slightly unstable, with enthalpy of formation of about $\Delta H \approx 22$ kJ/mol H_2, the most stable structure in the composition range (Mg:H = 2:1).

Among several possible ordered structures in the concentration range (Mg:H = 1:1), the most stable (although thermodynamically slightly unstable, with enthalpy of formation also about $\Delta H \approx 22$ kJ/molH_2) is the rutile structure containing two H-vacancies, indicating that the structural phase transition between the hcp lattice of Mg-metal and the bcc Mg sublattice of the rutile structure of MgH_2 takes place in this concentration range, or just below it. Indication of structural changes in this concentration range, manifested through the abrupt change of the Mg–H bond lengths were also noticed by the Mg–H clusters calculations [83]. By analyzing the structure of the competing phases DOS's in this concentration range (Figure 4), one can see that the metastable Wurtzite structure is

much more similar to the final rutile MgH_2 structure. This suggests that the transformation path of hcp-Mg to rutile MgH_2, upon hydrogenation, is not predisposed solely by thermodynamic conditions, and that some particular steps of the process could be controlled by appropriate (perhaps symmetry induced) transformation of electronic structure. The substoichiometric Mg–H rutile structures becomes thermodynamically stable at the concentration range of about Mg:H = 3:2, with enthalpy of formation of Mg_3H_2 of $\Delta H \approx -14$ kJ/molH_2.

Figure 4. Crystal structure, and Density of states (DOS), of (top to bottom): rutile MgH_2, MgH with NiAs structure, MgH with Wurtzite structure and Mg_2H with CdI_2 crystal structure (red spheres: Mg; blue spheres: H atoms).

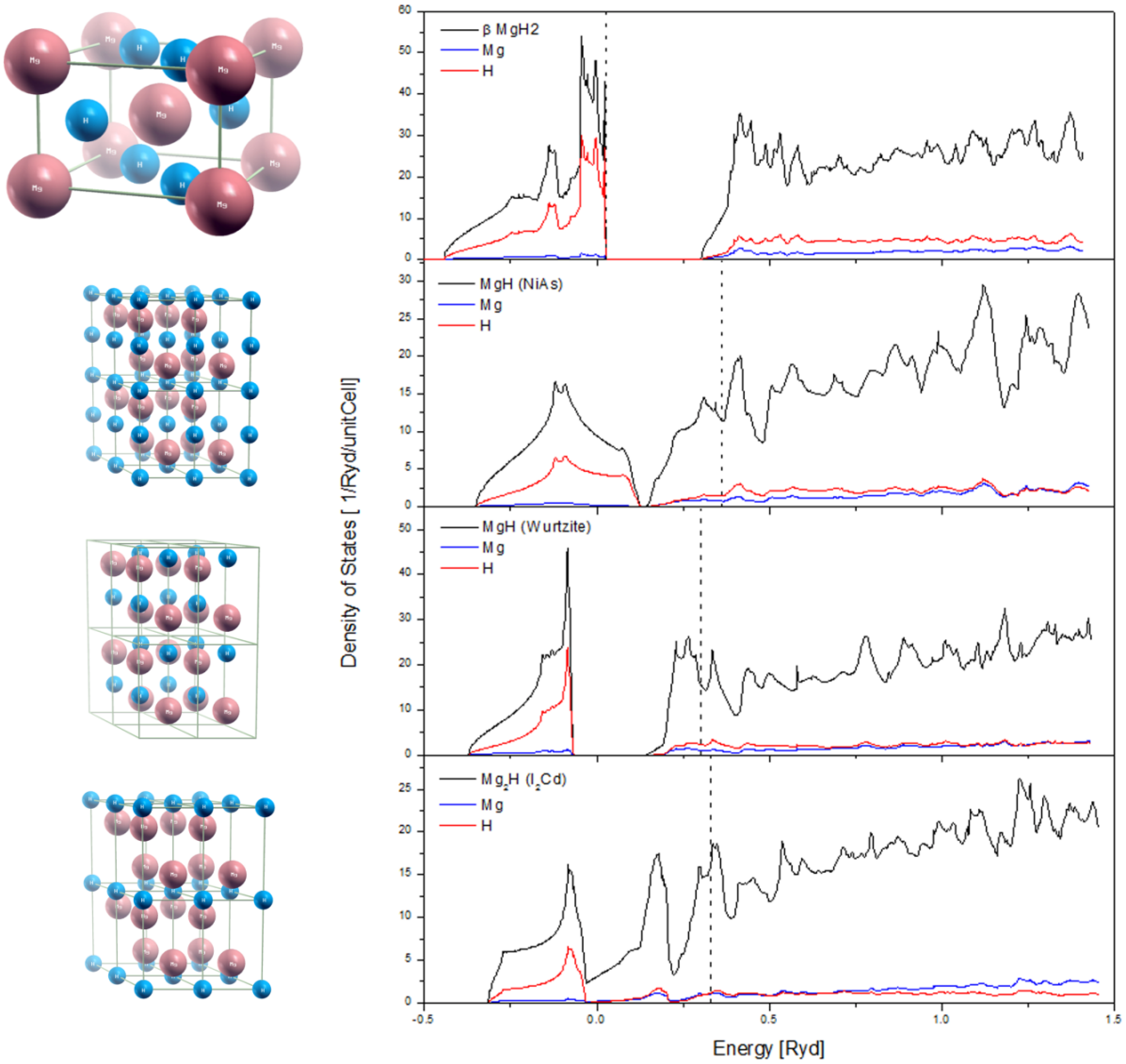

The presented results provide quite a detailed picture of the most important stages of the Mg structure transformation during hydrogenation. If true, they imply some serious consequences on H absorption kinetics. For instance, the finding that H prefers accommodation in particular (almost) ordered structures, that some of them are not the most convenient thermodynamically, and that they cannot be reached using stohastic diffusion paths (as proposed in [37,50]), imposes strong limitations

on H absorption kinetics. Also, the same discards all kinetic models of H absorption which consider the movement of the Mg/MgH_2 interface as the limiting step, because this interface does not form until at least (if ever) the Mg:H = 1:1 concentration range. Of course, the mentioned calculations have been performed at T = 0 K, they do not include the zero point, anharmonicity, and perhaps the quantum tunneling effects, which all could be important for hydrogen behavior.

The processes connecting the particular steps considered above also have not been explicitly accounted for, and some more knowledge about them could be obtained from the reverse process of MgH_2 dehydrogenation that is addressed in the next chapter.

2.4. Desorption of H (H_2) from MgH_2, and Its Decomposition during Dehydrogenation

We shall start the analysis of the MgH_2 dehydrogenation process by investigation of H (H_2) desorption from the most stable MgH_2 (110) and MgH_2 (001) surfaces. The structure and charge density distribution of the MgH_2 (110) surface system is presented in Figure 5

Figure 5. Structure and valence charge density of the MgH_2 (110) surface system. The cross-section through the plane perpendicular to (110) surface plane (original (001)) is presented. Red-Green-Blue color scale was used, ranging from red for low to blue for high electron density.

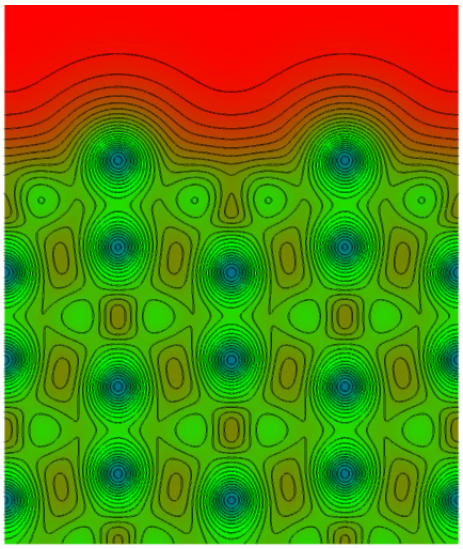

The activation barrier for H desorption was calculated [84] to be about 1.78 eV for the MgH_2 (110), and about 2.8 eV for the (001) surface Similar activation energies for H desorption from both considered surfaces were found also in [85].

These energies are higher than those obtained for various H vacancies formations, ranging from 1.3 to 1.6 eV [86], diffusion on the MgH_2 (110) surface (ranging from 0.15 to 0.80 eV), and from the surface into the bulk (ranging from 0.45 to 0.70 eV). Despite somewhat larger values obtained for defects formation and diffusion in [87], it is H desorption from the MgH_2 surfaces that is usually considered [88,89] as the rate-limiting step for dehydrogenation process of MgH_2. The common, and to a great extent, correct explanation for this is a strong ionic interaction between Mg and H. But, as can be seen in Figure 6a, besides the bonding between Mg (red spheres) and H (blue spheres), H–H

bonding interaction also exists in the system (see also Figure 3b in [84]). It is also clearly visible in Figure 6b, in the (110) crystallographic plane. The bonding H–H interaction is a rare appearance in metal hydrides, which certainly considerably hampers the H desorption kinetics from MgH_2.

Figure 6. (**a**) The unit cell of the MgH_2 rutile structure with bond critical points [90] denoted as small black spheres. Mg-red spheres, H-blue spheres. (**b**) The valence charge distribution in the bulk MgH_2 (110) crystallographic plane.

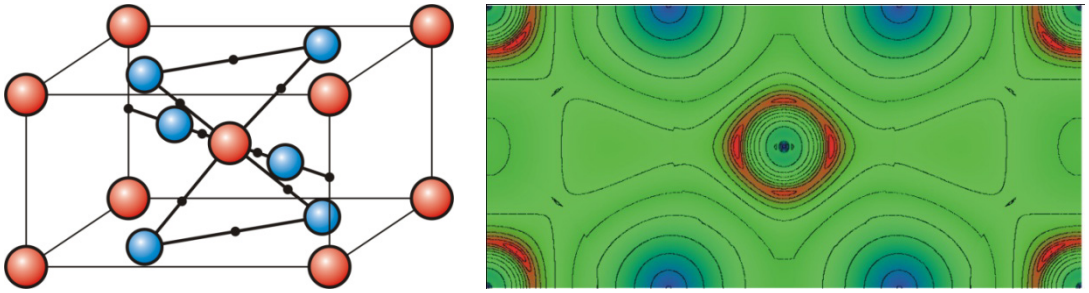

A **B**

It should be also remembered that conditions on the MgH_2 desorption surface changes substantially during the process, both due to depletion of the surface, and, in a more severe way, due to the structural phase transitions which should be expected for concentrations around Mg:H = 1:1 and below. One attempt in this direction is presented in Figure 7a,b, illustrating the H-desorption from the MgH_2 (110) surface, and the energy changes of the (fully relaxed) surface during the particular stages of the process.

Figure 7. (**a**) Illustration of successive H desorption from the MgH_2 (110) surface; (**b**) Desorption energy change of the relaxed MgH_2 (110) surface during the H desorption (blue spheres: Mg; red spheres: H atoms; arrows: directions and intensities of relaxation).

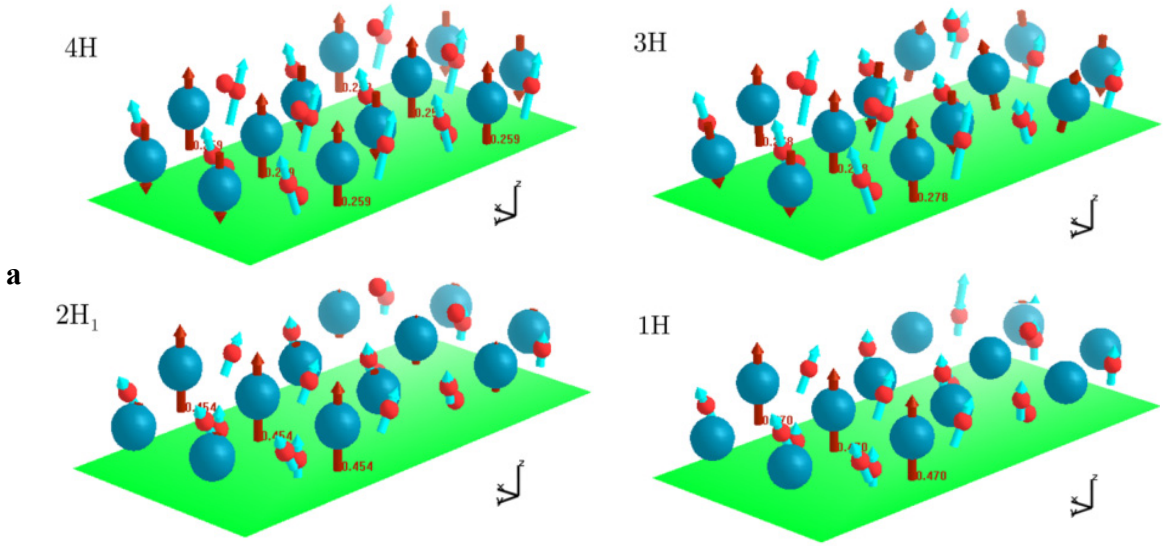

Figure 7. *Cont.*

b

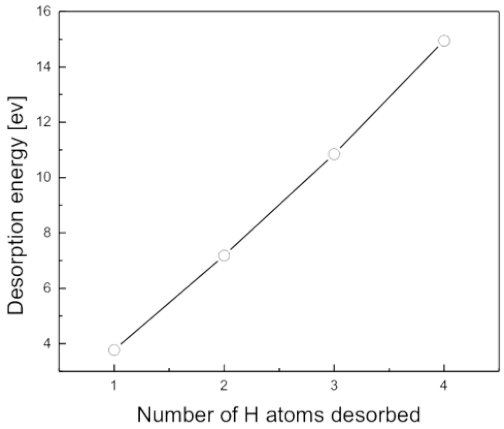

Although all mentioned [80,82,85–89,91,92] and other numerous investigations deal with only some particular aspects of the process (e.g., distinct points on the MgH_2 dehydrogenation curve), they are accurate enough to justify the expectation that the entire process (as well as the process of Mg hydrogenation) will be resolved "from the first principles" in the near future. Also, the investigations have "located'' the main obstacles that should be resolved in the further attempts to improve the performances of the Mg–H system. Some possibilities for that are discussed in the following chapter.

2.5. Possibilities for Improvement of the Mg/MgH_2 Hydrogenation/Dehydrogenation Performances

As we mentioned previously, practical applications of metal hydrides for H storage require strict conditions to be fulfilled [1,2,5,9–14]: H absorption/desorption at moderate temperatures and pressures, reversibility of cycling, material stability under operating conditions, large H-uptake, low weight, reasonable price, and so on. Obviously, it is difficult to find the material that can satisfy all these requirements at the same time, and for that reason a huge amount of various systems have been investigated.

The most improvements have come from the catalytic approaches, in which the size of the MgH_2 particles have been reduced down to the nanometer dimensions (increasing the surface/volume ratio), their surface made more active and (or) the bulk less ordered by introduction of defects of various kinds, and by adding various elements to the system, molecules and compounds [3,4,6–8,41,44,53–64,93,94]. All above mentioned approaches could be understood and its particular relation to H-behavior resolved and established from the electronic structure point of view. The influence of more open, or more dense, metal surfaces and bulk structures on H accommodation has been briefly mentioned in previous chapters, and the importance of surface defects has been also recognized [77]. Simply speaking, any dilution of the metal structure (for instance with defects) would in principle lead to a charge density structure which is more convenient for H accommodation, and its trapping [78]. If the diffusion barrier between different defects or between defects and interstices is lower than between the interstices themselves, defects could facilitate H mobility in the system, but the opposite scenario is also possible.

Although it is generally true for all defects, the effects of impurity atoms on H-behavior in the system depend essentially on their electronic structure. Here we will briefly outline the influence of transition metal (TM) impurities on the Mg/MgH_2 system properties. Extensive

experimental [3,4,6–8,44,55–62] and theoretical (computational) [21,44,67–72,91,93–98] investigations have been devoted to the subject, and the importance of the TM(d)–H(s) interaction for the TM catalytic properties [67,71,72,93,95,96] established. To illustrate this, the difference between the center of the TM 3d-band and H(s) level, and its position relative to the 3d-band [99], are presented in Figure 8. The figure shows how the H(s) level taken as a zero energy level, enters and leaves the 3d band while moving along the series.

The consequence of such behavior is an increase of electron density around TM impurity, and therefore an increase of strength of TM–H bonding (reflected in the shortening of the TM–H bond). The trend is visible while moving from Ti to Fe, and eventually could be violated if magnetic interaction in the system becomes important [70,91]. Further filling of the d-band going from Co to Ni and on (Cu, Zn) leads to gradual movement of Fermi level (E_F) away from the center of the d-band, and the ongoing population of the H(s*) anti-bonding level. This leads to weakening of the TM–H interaction and to expansion of the TM-H bond length [70]. The existence of such a clear trend implies that single TM impurity could not satisfy all requirements (adsorption, dissociation, diffusion into and from the bulk and desorption) necessary to improve the H-sorption kinetics of the Mg/MgH_2 system. Indeed, both experimental (for instance [4] and [59]), and calculation results are often inconsistent. For instance, in ref. [4] it has been found that among the TM of the 3d-series Ti and V improve the most, and Ni the least, both absorption and desorption properties of Mg/MgH_2 among the TM of the 3d-series, and [59] claims that Ni is a much better catalyst than Fe and Co. A recent computational study [93] predicts that all 3d TM when absorbed at the Mg (0001) surface induce dissociation of H_2, but that Ti and V provide much slower H-absorption kinetics, than for instance Mn, Fe and Co.

The reason for these discrepancies could be major differences in performed experimental conditions (milling time and energy, particle size, formation of stable TM-hydrides and other "parasitic" phases, *etc.*), measuring techniques and conditions and the used computational methods.

Figure 8. Dependence of the relative position of the 3d-band zone center and the H(s) level, and the half of the d-band width along the 3d-series.

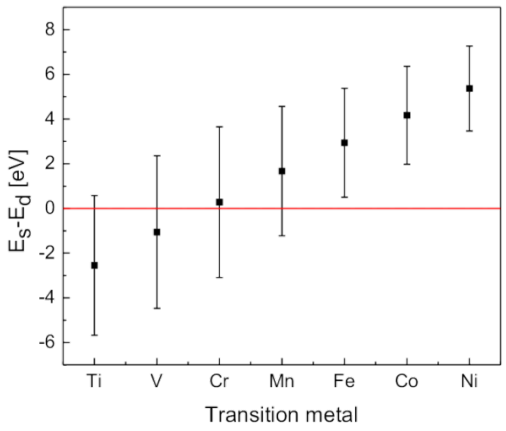

However, the fact that all details of the catalytic mechanism of TM in Mg/MgH_2 are still not adequately explained also deserves consideration. For instance, it has been found [71] that catalytic properties of TM in Mg–H clusters strongly depend on its environment (edge, surface, or bulk) in

different ways for different TM impurities. It has been also shown [70,72] that TM impurities exhibit a different behavior in different crystal structures of the Mg–H system

An interesting insight in influence of Ti and Co impurity (10 wt.%) on the MgH_2 rutile structure is presented in [72,91]. In Figure 9, the valence charge distributions around Ti and Co impurity in (110) plane are presented.

The charge distributions around Ti and Co atoms are quite different, both being of predominantly t_{2g} character. Around Ti it is however directed between the neighboring H atoms, and around Co it is more spherical, with significant contribution of charge directed toward the H atoms. Both Ti and Co interact with four neighboring H atoms in (110) plane, but also in (−1−10) plane where the interaction is extended from the two nearest neighbor H toward the two H in the third coordination of TM. In Table 1, one can see that Co–H bond length is shorter than Ti–H one, but that Co destabilize the MgH_2 structure more than Ti. It has been also found that magnetic interaction in the MgH_2:Co system affords an important contribution to the ground state energy of the system.

Figure 9. Valence charge density of (**a**) MgH_2:Ti and (**b**) of MgH_2:Co in (110) plane.

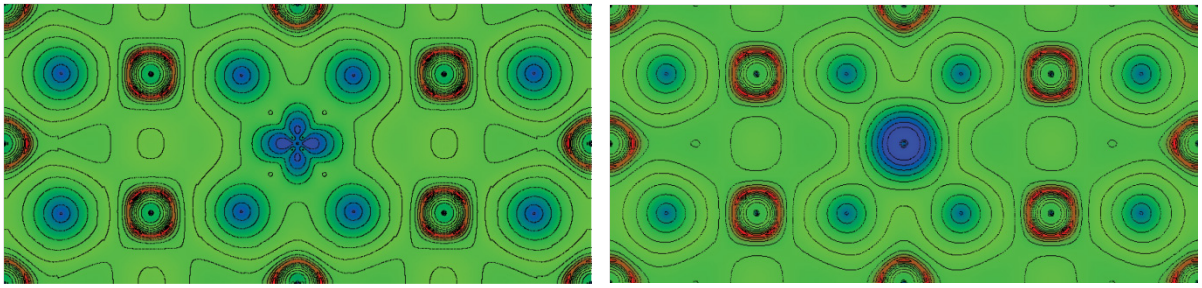

A **B**

Table 1. Calculated results of structural optimization, total energies, and heats of formation, of MgH_2, MgH_2:Ti, MgH_2:Co.

Compound	Distances [Å]					E_{tot}	ΔH
	Atom	nn H4	nn H2	nn Mg	nnn H		
MgH_2	Mg	1.952	1.953	3.019	3.424	−806.08	−69.51
MgH_2:Ti	Ti	1.916	1.905	3.041	3.440	−7755.53	−60.64
MgH_2:Co	Co	1.789	1.802	3.025	3.458	−8834.79	−53.23

nn: nearest neighbor; nnn: next nearest neighbor.

One possible explanation why Co destabilizes MgH_2 more than Ti could be that strong local TM–H interaction weakens the rest of the bonds in the compound due to the strong localization of the valence charge in the first coordination of TM more around Co than around Ti. If this hypothesis is correct, it should be reflected in the H-desorption kinetics from these systems which, after the initial acceleration, could slow down for the H-poor phases.

It should be mentioned here that a consistent explanation of TM hydrides formation and stability is challenging in itself [21,91,96], and this is particularly true for hydrides of complex intermetallic compounds [100–103].

The established fact that some local structures inside the very same unit cell of the complex compounds of the Ti_2Ni structure type are much more susceptible to H absorption than others [104,105],

should be due to remarkably different charge topology observed at different lattice positions in some of these systems [106].

Although the large specific weight prevent their practical applications as H-storage materials, the fact that their electronic properties, and consequently the environment for H-uptake could be altered considerably inside the same structure by changing the constitutive elements of the compound [107,108], provides a valuable example of how to adjust the local electronic charge distribution inside a complicated system, which could be of importance for understanding another type of complex hydrides presented in the next chapter.

2.6. Few Words about "Modern" Complex Hydrides

After the first encouraging results with alanates [27–29], a large variety of complex metal hydrides [25,30–32,107–112] have been considered as potential candidates for hydrogen storage. These are usually materials with complicated crystal structures in which H is accommodated in specific clusters or molecules. In these materials the process of H absorption/desorption is often accompanied and promoted by structural phase transitions, improving the kinetics, and enabling the processes to take place under favorable thermodynamic conditions. Together with the small specific weight and large hydrogen uptake, this makes these materials (various alanates, amides-imides, borohydrides *etc*.) promising candidates for practical applications. As a representative of kind, we will shortly consider the reversible $LiNH_2$ (Li-amide) to Li_2NH (Li-imide) transformation, which recently attracted considerable interest in the scientific community [30–32,109,113].

In Figure 10a the $LiNH_2$ crystal structure (space group I-4), in Figure 10b the charge distribution in the $LiNH_2$ (110) plane and in Figure 10c, one of the several possible Li_2NH crystal structures (space group Im2m) is presented.

Figure 10. (**a**) the $LiNH_2$ crystal structure (space group I-4) (grey spheres: Li; red spheres: N; blue spheres: H atoms); (**b**) the charge distribution in the $LiNH_2$ (110) plane; (**c**) one of the several possible Li_2NH crystal structures (space group Im2m) (blue spheres: Li; red spheres: N; grey spheres: H atoms).

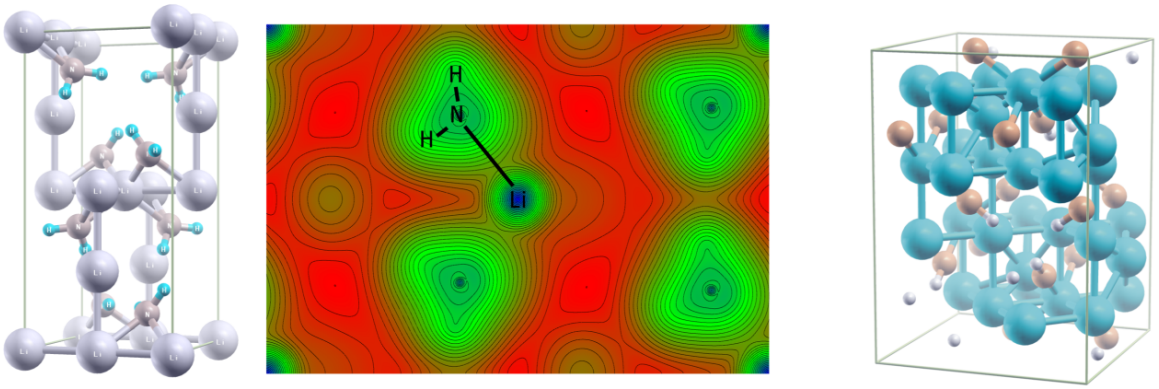

a) b) c)

It has been found [32] that $LiNH_2$ crystal structure induces considerable elongation of the Li–N bond in $LiNH_2$ molecule, which increase energy of the molecule, and soften some of the molecular

vibrational modes. This makes detachment of H fast at temperatures around 250 °C [30] (which are likely to be lower by addition of suitable impurities, like Mg [31]), and structure changes to Li_2NH. The ground state structure of Li_2NH was a subject of considerable debate, and it seems [26] that quantum effects enable the H-diffusion among available crystal positions stabilizing the Fd-3m structure at low temperatures, which changes into anti-fluorite Fm-3m phase at about 360 K [114]. Perhaps the same effect is responsible for the existence of numerous metastable phases [113] with very close ground state energies, which could also play a role in the Li-amide/imide transformation process, opening numerous channels for hydrogen desorption. Similar mechanisms were found also in some other "modern" complex hydrides, encouraging investigation of structures and structural transformations, which could manage H sorption, and not just follow it.

3. Summary and Perspectives

In this article we have made an attempt to describe numerous phenomena observed in metal hydrides by means of electronic structure and interactions. The major intention was to provide a clear, as simple as possible ("...but not simpler" A. Einstein) physical picture rather than quoting numerous, sometimes complicated details of experiments, theory and computations. For this reason, we have started with the Effective Medium Theory (EMT), of Nørskov *et al*. [97], which gives a simple, transparent and in many cases quite accurate explanation of H-behavior in metallic systems. The theory shows in a straightforward manner how the charge density distribution of the metal host influence H_2 adsorption, dissociation, H positioning on the surface, its diffusion into the bulk and accommodation in specific crystal structures (like interstices).

As the theory relies on charge density properties alone, it enables one to predict H interaction with any physical entity (surface, defect, impurity,...), if principle features of the charge density are somehow determined, which is of great help in explaining numerous experimental findings that exist for metal hydrides.

Moreover, in cases where this simple theory is not good enough, it gives direction for improvement, taking into account the perturbations induced by H-host interaction, ions polarizabilities, specific energy level interactions, and so on. Although most of the calculation results presented in this article have been obtained by *ab initio* calculations, EMT and other "simple" theories (such as the tight-binding theory), they are indispensable for the explanation of real physical system results.

Concerning specific metal hydrides, the most attention is given to the Mg–H system. This is considered to be among the most perspective ones, with a huge amount of various data, which allowed us to illustrate our approach to metal hydrides in a detailed and consistent manner. We briefly analyze all stages of Mg–H interaction using ours and other authors results (H_2 absorption and dissociation on the Mg (0001) surface, H positioning on the surface, its diffusion and accommodation in the bulk, formation of various (meta) stable phases and *vice versa*, H desorption from the MgH_2 surface and further dehydrogenation) . In this way, all relevant steps of H absorption/desorption in Mg/MgH_2 system and their role in H sorption kinetics have been explained from the first principles.

One of these opportunities, alloying with 3d transition metal (TM) elements, is explored in some detail, pointing out the importance of relative position and the width of the 3d band in interaction with H(s) bonding and antibonding state. We also mention the fact that the strength of the TM–H interaction

in MgH_2 is not directly correlated with the stability of the corresponding TM hydrides. The remarkable property of some complex intermetallic compounds, which absorb H around particular positions in the crystal lattice having homogenous charge distribution (low electric field gradient, EFG), but not around the others positions in the very same unit cell having highly inhomogenous charge distribution (large EFG), has also been reported. Although these compounds are not promising candidates for H-storage applications, the observed phenomenon helps us to learn how to design unique systems where H will be placed into one type of crystallographic sites, and swiftly moved along the network of the other type of crystallographic positions.

Several interesting results were found concerning "modern" complex hydrides (alanates, amides/imides, borohydrides), and they are explained from the point of view of hydrogen sorption driven (or simply accompanied) by structural phase transformations.

This article offers an approach for further investigation and improvement of metal hydrides properties based on fundamental principles of electronic structures and interactions. We expect that the other perspective metal-hydrogen systems and phenomena observed in them will be treated in a similar way as the Mg–H system, e.g., by investigating the electronic structure of all the relevant stages and processes in them. As could be seen from the examples given in this article, but also from the numerous stated references, knowledge how the charge density features influence H-behavior, and how we could adjust it, in principle already exists. However, many details of the metal–hydrogen interaction still need to be explored, particularly for complex hydrides with many atoms per unit cell, and in cases where the phase transitions are essential for understanding the process.

The necessary tools are already available. The new generation of synchrotron installations provides photon sources of tremendous brightness over a broad range of frequencies, introducing new measuring techniques in real time. Development of microscopy with atomic resolution, and new improved neutron sources also gives hope for better experimental results.

Computation methods have also made significant progress, not only owing to the faster machines and improved codes, but also due to some original approaches to results interpretation. Bader analysis of the charge distribution topology have already provided some interesting results, for instance that LiH has significantly different distribution of bond critical points than other alkali metal hydrides, explaining its quite different macroscopic characteristics, and that bonding points exist between certain pairs of H in MgH_2, giving additional reasons for high barrier of H desorption. A similar scenario is true for the electron localization function (ELF) and crystal orbital Hamilton population (COHP) methods, which provided several illuminating results about metal hydrides.

Bearing in mind all the information presented, it is reasonable to expect that existing knowledge and possibilities to improve it will afford progress in metal hydride design in the near future, significant enough to facilitate their practical applications.

Acknowledgments

This paper is financially supported by Serbian Ministry of Education and Science under grant III45012

Conflict of Interest

The authors declare no conflict of interest.

References

1. Schlapbach, L.; Zuttel, A. Hydrogen-storage materials for mobile applications. *Nature* **2001**, *414*, 353–358.
2. Zuttel, A. Materials for hydrogen storage. *Mater. Today* **2003**, *6*, 24–33.
3. Bobet, J.-L.; Even, C.; Nakamura, Y.; Akiba, E.; Darriet, B. Synthesis of magnesium and titanium hydride via reactive mechanical alloying. Influence of 3D-metal addition on MgH_2 synthesize. *J. Alloys Compounds* **2000**, *298*, 279–284.
4. Liang, G.; Huot, J.; van Neste, A.; Schulz, R. Catalytic effect of transition metals on hydrogen sorption in nanocrystalline ball milled MgH_2-Tm (Tm = Ti, V, Mn, Fe and Ni) systems. *J. Alloys Compounds* **1999**, *292*, 247–252.
5. Jain, I.P.; Lal, Ch.; Jain, A. Hydrogen storage in Mg: A most promising material. *Int. J. Hydrogen Energy* **2010**, *35*, 5133–5144.
6. Liang, G.; Schulz, R. Synthesis of Mg–Ti alloy by mechanical alloying. *J. Mater. Sci*. **2003**, *38*, 1179–1184.
7. Zaluski, L.; Zaluska, A.; Strom-Olsen, J.O. Nanocrystalline metal hydrides. *J. Alloys Compounds* **1997**, *253–254*, 70–79.
8. Bassetti, A.; Bonetti, E.; Pasquini, L.; Montone, A.; Grbovic, J.; Vittori Antisari, M. Hydrogen desorption from ball milled MgH_2 catalyzed with Fe. *Eur. Phys. J. B* **2005**, *43*, 19–27.
9. Gupta, R.B. *Hydrogen Fuel Production Transport and Storage*, 1st ed.; CRC Press: Boca Raton, FL, USA, 2009.
10. Varin, R.A.; Czujko, T.; Wronski, Z.S. *Nanomaterials for Solid State Hydrogen Storage*, 1st ed.; Springer Science Bussines Media: New York, NY, USA, 2009.
11. Hirscher, M. *Handbook of Hydrogen Storage: New Materials for Future Energy Storage*, 1st ed.; Wiley-VCH Verlag GmbH & Co. KgaA: Weinheim, Germany, 2010.
12. Walker, G. Solid-state hydrogen storage. In *Materials and Chemistry*, 1st ed.; Woodhead Publishing Limited: Cambridge, UK, 2008.
13. Fukai, Y. *The Metal–Hydrogen System*, 2nd ed.; Springer: Berlin, Germany, 2005.
14. Borgschulte, A.; Schlapbach, L. *Hydrogen as A Future Energy Carrier*; 1st ed.; Zuttel, A., Ed.; Wiley-VCH Verlag GmbH & Co. KgaA: Weinheim, Germany, 2008.
15. Bowman, R.C. Cohesive energies of the alkali hydrides and deuterides. *J. Phys. Chem.* **1971**, *75*, 1251–1255.
16. Luaña, V.; Pueyo, L. Simulation of ionic crystals: The *ab initio* perturbed-ion method and application to alkali hydrides and halides. *Phys. Rev. B* **1990**, *41*, 3800–3814.
17. Wolverton, C.; Ozoliņš, V.; Asta, M. Hydrogen in aluminum: First-principles calculations of structure and thermodynamics. *Phys. Rev. B* **2004**, *69*, 144109:1–144109:16.

18. Vidal-Valat, G.; Vidal, J.-P.; Kurki-Suonio, K.; Kurki-Suonio, R. Evidence on the breakdown of the Born-Oppenheimer approximation in the charge density of crystalline 7LiH/D. *Acta Cryst.* **1992**, *A48*, 46–60.
19. Blat, D.K.; Zein, N.E.; Zinenko, V.I. Calculations of phonon frequencies and dielectric constants of alkali hydrides via the density functional method. *J. Phys. Condens. Matter* **1991**, *3*, 5515–5524.
20. Ivanović, N.; Novaković, N.; Colognesi, D.; Radisavljević, I.; Ostojić, S. Electronic principles of some trends in properties of metallic hydrides. *Int. J. Mod. Phys. B* **2010**, *24*, 703–710.
21. Smithson, H.; Marianetti, C.A.; Morgan, D.; van der Ven, A.; Predith, A.; Ceder, G. First-principles study of the stability and electronic structure of metal hydrides. *Phys. Rev. B* **2002**, *66*, 144107:1–144107:10.
22. Lebegue, S.; Alouani, M.; Arnuad, B.; Pickett, W.E. Pressure-induced simultaneous metal-insulator and structural-phase transitions in LiH: A quasiparticle study. *Europhys. Lett.* **2003**, *63*, 562–568.
23. Novaković, N.; Radisavljević, I.; Colognesi, D.; Ostojić, S.; Ivanović, N. First principle calculations of alkali hydride electronic structures. *J. Phys. Condens. Matter* **2007**, *19*, 406211:1–406211:14.
24. Vajeeston, P. Theoretical Modeling of Hydrides. Ph.D. Thesis, University of Oslo, Oslo, Norway, 2004.
25. Ravindran, P.; Vajeeston, P.; Fjellvåg, H.; Kjekshus, A. Chemical-bonding and high-pressure studies on hydrogen-storage materials. *Comput. Mater. Sci*. **2004**, *30*, 349–357.
26. Ceriotti, M.; Miceli, G.; Pietropaolo, A.; Colognesi, D.; Nale, A.; Catti, M.; Bernasconi, M.; Parrinello, M. Nuclear quantum effects in *ab initio* dynamics: Theory and experiments for lithium imide. *Phys. Rev*. *B* **2010**, *82*, 174306:1–174306:5.
27. Bogdanović, B.; Schwickardi, M. Ti-doped alkali metal aluminium hydrides as potential novel reversible hydrogen storage materials. *J. Alloys Compounds* **1997**, *253–254*, 1–9.
28. Bogdanović, B.; Brand, R.A.; Marjanović, A.; Schwickardi, M.; Tölle, J. Metal-doped sodium aluminium hydrides as potential new hydrogen storage materials. *J. Alloys Compounds* **2000**, *302*, 36–58.
29. Vajeeston, P.; Ravindran, P.; Vidya, R.; Fjellvåg, H.; Kjekshus, A. Pressure-induced phase of NaAlH4: A potential candidate for hydrogen storage? *Appl. Phys. Lett.* **2003**, *82*, 2257–2259.
30. Chen, P.; Xiong, Z.; Luo, J.; Lin, J.; Tan, K.L. Interaction of hydrogen with metal nitrides and imides. *Nature* **2002**, *420*, 302–304.
31. Luo, W.; Rönnebro, E. Towards a viable hydrogen storage system for transportation application. *J. Alloys Compounds* **2005**, *404–406*, 392–359.
32. Ivanović, N.; Radisavljević, I.; Novaković, N.; Manasijević, M.; Colognesi, D. Calculations of molecular structures and processes important for hydrogen behaviour in the Li-amide/imide system. *Acta Phys. Pol.* **2011**, *119*, 242–245.
33. Dyck, W.; Jex, H. Lattice dynamics of alakali hydrides and deuterides with the NaCl type structure. *J. Phys. C Solid State Phys.* **1981**, *14*, 4193–4215.
34. Yu, R.; Lam, P.K. Electronic and structural properties of MgH_2. *Phys. Rev. B* **1988**, *37*, 8730–8737.
35. Kunz, A.B.; Mickish, D.J. Electronic structure of LiH and NaH. *Phys. Rev. B* **1975**, *11*, 1700–1704.

36. Grosso, G.; Parravicini, G.P. Hartree-Fock energy bands by the orthogonalized-plane-wave method: Lithium hydride results. *Phys. Rev. B* **1979**, *20*, 2366–2372.
37. Zeng, K.; Klassen, T.; Oelerich, W.; Bormann, R. Critical assessment and thermodynamic modeling of the Mg–H system. *Int. J. Hydrogen Energy* **1999**, *24*, 989–1004.
38. Miademma, A.R. The electronegativity parameter for transition metals: Heat of formation and charge transfer in alloys. *J. Less Common Metals* **1973**, *32*, 117–136.
39. Rao, B.K.; Jena, P. Switendick criterion for stable hydrides. *Phys. Rev. B* **1985**, *31*, 6726–6730.
40. Sakintuna, B.; Lamari-Darkrim, F.; Hirscher, M. Metal hydride materials for solid hydrogen storage: A review. *Int. J. Hydrogen Energy* **2007**, *32*, 1121–1140.
41. Bazzanella, N.; Checchetto, R.; Miotello, A. Catalytic effect on hydrogen desorption in Nb-doped microcrystalline MgH_2. *Appl. Phys. Lett*. **2004**, *85*, 5212–5214.
42. Schimmel, H.G.; Johnson, M.R.; Kearley, G.J.; Ramirez-Cuesta, A.J.; Huot, J.; Mulder, F.M. Structural information on ball milled magnesium hydride from vibrational spectroscopy and *ab initio* calculations. *J. Alloys Compounds* **2005**, *393*, 1–4.
43. Gross, K.J.; Chartouni, D.; Leroy, E.; Zuttel, A.; Schlapbach, L. Mechanically milled Mg composites for hydrogen storage: The relationship between morphology and kinetics. *J. Alloys Compounds* **1998**, *269*, 259–270.
44. Grbović Novaković, J.; Brdarić, T.; Novaković, N.; Matović, Lj.; Montone, A.; Mentus, S. Experimental and theoretical investigation of hydrogen storage magnesium based composites. *Mat. Sci. Forum* **2007**, *555*, 343–348.
45. Matović, Lj.; Novaković, N.; Kurko, S.; Šiljegović, M.; Matović, B.; Romčević, N.; Kačarević-Popović, Z.; Ivanović, N.; Grbović Novaković, J. Structural destabilisation of MgH_2 obtained by heavy ion irradiation. *Int. J. Hydrogen Energy* **2009**, *34*, 7275–7282.
46. Grbović Novaković, J.; Matović, Lj.; Milovanović, S.; Drvendžija, M.; Novaković, N.; Rajnović, D.; Šiljegović, M.; Kačarević-Popović, Z.; Ivanović, N. Changes of hydrogen storage properties of MgH_2 induced by heavy ion irradiation. *Int. J. Hydrogen Energy* **2008**, *33*, 1876–1879.
47. Westerwaal, R.J.; Broedersz, C.P.; Gremaud, R.; Slaman, M.; Borgschulte, A.; Lohstroh, W.; Tscherisch, K.G.; Fleischhauer, H.P.; Dam, B.; Griessen, R. Study of the hydride forming process of *in situ* grown MgH_2 thin films by activated reactive evaporation. *Thin Solid Films* **2008**, *516*, 4351–4359.
48. Stander, C.M.; Pacey, R.A. The lattice energy of magnesium hydride. *J. Phys. Chem. Solid* **1978**, *39*, 829–832.
49. Noritake, T.; Aoki, M.; Towata, S.; Seno, Y.; Hirose, Y.; Nishibori, E.; Takata, M.; Sakata, M. Chemical bonding of hydrogen in MgH_2. *Appl. Phys. Lett.* **2002**, *81*, 2008–2010.
50. Schimmel, H.G.; Kearley, G.J.; Huot, J.; Mulder, F.M. Hydrogen diffusion in magnesium metal (α phase) studied by *ab initio* computer simulations. *J. Alloys Compounds* **2005**, *404–406*, 235–237.
51. Kelkar, T.; Kanhere, D.G.; Pal, S. First principles calculations of thermal equations of state and thermodynamical properties of MgH_2 at finite temperatures. *Comput. Mat. Sci.* **2008**, *42*, 510–516.

52. Ares, J.R.; Leardini, F.; Díaz-Chao, P.; Bodega, J.; Fernández, J.F.; Ferrer, I.J.; Sánchez, C. Ultrasonic irradiation as a tool to modify the H-desorption from hydrides: MgH_2 suspended in decane. *Ultrason. Sonochem.* **2009**, *16*, 810–816.
53. Imamura, H.; Yoshihara, K.; Yoo, M.; Kitazawa, I.; Sakata, Y.; Ooshima, S. Dehydriding of Sn/MgH_2 nanocomposite formed by ball milling of MgH_2 with Sn. *Int. J. Hydrogen Energy* **2007**, *32*, 4191–4194.
54. Pfrommer, B.; Elasässer, C.; Fähnle, M. Possibility of Li–Mg and Al–Mg hydrides being metallic. *Phys. Rev. B* **1994**, *50*, 5089–5093.
55. Montone, A.; Grbović, J.; Stamenković, Lj.; Fiorini, A.L.; Pasquini, L.; Bonetti, E.; Vittori Antisari, M. Desorption Behaviour in Nanostructured MgH_2–Co. *Mater. Sci. Forum* **2006**, *518*, 79–84.
56. Berlouis, L.E.A.; Cabrera, E.; Hall-Barientos, E.; Hall, P.J.; Dodd, S.B.; Morris, S.; Imam, M.A. Thermal analysis investigation of hydriding properties of nanocrystalline Mg–Ni- and Mg–Fe-based alloys prepared by high-energy ball milling. *J. Mater. Res.* **2001**, *16*, 45–57.
57. Montone, A.; Grbović, J.; Vittori Antisari, M.; Bassetti, A.; Bonetti, E.; Fiorini, A.L.; Pasquini, L.; Mirenghi, L.; Rotolo, P. Nano-micro MgH_2–Mg_2NiH_4 composites: Tayloring a multichannel system with selected hydrogen sorption properties. *Int. J. Hydrogen Energy* **2007**, *32*, 2026–2934.
58. Bassetti, A.; Bonetti, E.; Fiorini, A.L.; Grbovic, J.; Montone, A.; Pasquini, L.; Vittori Antisari, M. Microstructure and hydrogen desorption in nanostructured MgH_2–Fe. *Mater. Sci. Forum* **2004**, *453–454*, 205–212.
59. Hanada, N.; Ichikava, T.; Fujii, H. Catalytic effect of nanoparticle 3d-transition metals on hydrogen storage properties in magnesium hydride MgH_2 prepared by mechanical milling. *J. Phys. Chem. B* **2005**, *109*, 7188–7194.
60. Bobet, J.-L.; Akiba, E.; Nakamura, Y.; Darrie, B. Study of Mg–*M* (*M* = Co, Ni and Fe) mixture elaborated by reactive mechanical alloying—Hydrogen sorption properties. *Int. J. Hydrogen Energy* **2000**, *25*, 987–996.
61. Oelerich, W.; Klassen, T.; Bormann, R. Comparison of the catalytic effects of V, V_2O_5, VN and VC on the hydrogen sorption of nanocrystalline Mg. *J. Alloys Compounds* **2001**, *322*, L5–L9.
62. Gulicovski, J.; Rašković-Lovre, Ž.; Kurko, S.; Vujasin, R.; Jovanović, Z.; Matović, Lj.; Grbović Novaković, J. Influence of vacant CeO_2 nanostructured ceramics on MgH_2 hydrogen desorption properties. *Ceram. Int.* **2012**, *38*, 1181–1186.
63. Aguey-Zinsou, K.-F.; Ares Fernandez, J.R.; Klassen, T.; Bormann, R. Effect of Nb_2O_5 on MgH_2 properties during mechanical milling. *Int. J. Hydrogen Energy* **2007**, *32*, 2400–2407.
64. Sun, D.; Gingl, F.; Enoki, H.; Ross, D.K.; Akiba, E. Phase components of the sintered Mg–*X* wt.% $LaNi_5$ (*X* = 20–50) composites and their hydrogenation properties. *Acta Mater.* **2000**, *48*, 2363–2372.
65. Novaković, N.; Matović, Lj.; Grbović Novaković, J.; Manasijević, M.; Ivanović, N. *Ab Initio* Study of MgH_2 Formation. *Mater. Sci. Eng. B* **2009**, *165*, 235–238.
66. Borgschulte, A.; Gremaud, R.; Griessen, R. Interplay of diffusion and dissociation mechanisms during hydrogen absorption in metals. *Phys. Rev. B* **2008**, *78*, 094106:1–094106:16.
67. Du, A.J.; Smith, S.C.; Yao, X.D.; Lu, G.Q. The role of Ti as a catalyst for the dissociation of hydrogen on a Mg (0001) Surface. *J. Phys. Chem. B* **2005**, *109*, 18037–18041.

68. Song, Y.; Guo, Z.X.; Yang, R. Influence of selected alloying elements on the stability of magnesium dihydride for hydrogen storage applications: A first principle investigation. *Phys. Rev. B* **2004**, *69*, 094205:1–094205:11.
69. Shang, C.X.; Bououdina, M.; Song, Y.; Guo, Z.X. Mechanical alloying and electronic simulations of (MgH_2–*M*) systems (*M* = Al, Ti, Fe, Ni, Cu and Nb) for hydrogen storage. *Int. J. Hydrogen Energy* **2004**, *29*, 73–80.
70. Vegge, T.; Hedegaard-Jensen, L.S.; Bonde, J.; Munter, T.R.; Norskov, J.K. Trends in hydride formation energies for magnesium-3d transition metal alloys. *J. Alloys Compounds* **2005**, *386*, 1–7.
71. Larsson, P.; Moyses Araújo, C.; Larsson, J.A.; Jena, P.; Ahuja, R. Role of catalysts in dehydrogenation of MgH_2 nanoclusters. *Proc. Natl. Acad. Sci. USA* **2008**, *105*, 8227–8231.
72. Novaković, N.; Grbović Novaković, J.; Matović, Lj.; Manasijević, M.; Radisavljević, I.; Paskaš-Mamula, B.; Ivanović, N. *Ab initio* calculations of MgH_2, MgH_2:Ti and MgH_2:Co compounds. *Int. J. Hydrogen Energy* **2010**, *35*, 598–608.
73. Blaha, P.; Schwarz, K.; Madsen, G.K.H.; Kvasnicka, D.; Luitz, J. *WIEN2k*, *An Augmented Plane Wave+Local Orbitals Program for Calculating Crystal Properties*; Karlheinz Schwarz, Techn. Universtät: Wien, Austria, 2001.
74. Nørskov, J.L.; Lang, N.D. Effective-medium theory of chemical binding: Application to chemisorptions. *Phys. Rev. B* **1980**, *21*, 2131–2136.
75. Puska, M.J.; Nieminen, R.M. Atoms embedded in an electron gas: Beyond the local-density approximation. *Phys. Rev. B* **1991**, *43*, 12221–12233.
76. Nieminen, R.M.; Puska, M.J.; Mannienen, M. *Many-Atom Interactions in Solids (Springer Proceedings in Physics*); Springer-Verlang: Berlin/Heidelberg, Germany, 1990; Volume 48.
77. Nørskov, J.K.; Houmøller, A.; Johansson, P.K.; Lundquist, B.I. Adsorption and dissociation of H_2 on Mg surface. *Phys. Rev. Lett*. **1981**, *46*, 257–260.
78. Nørskov, J.K.; Besenbacher, F.; Bøttiger, J.; Nielsen, B.B.; Pisarev, A.A. Interaction of hydrogen with defects in metals: Interplay between theory and experiment. *Phys. Rev. Lett.* **1982**, *49*, 1420–1423.
79. Gonze, X.; Amadon, B.; Anglade, P.-M.; Beuken, J.-M.; Bottin, F.; Boulanger, P.; Bruneval, F.; Caliste, D.; Caracas, R.; Cote, M., *et al*. ABINIT: First-principles approach of materials and nanosystem properties. *Comp. Phys. Commun.* **2009**, *180*, 2582–2615.
80. Wu, G.; Liu, S.; Zhang, J.; Wu, Y.; Chou, K.; Bao, X. Density functional theory study on hydrogenation mechanism in catalyst-activated Mg (0001) surface. *Trans. Nonferrous Met. Soc. China* **2009**, *19*, 383–388.
81. Sprunger, P.T.; Plummer, E.W. An experimental study of the interaction of hydrogen with the Mg (0001) surface. *Chem. Phys. Lett.* **1991**, *187*, 559–564.
82. Johansson, M.; Ostenfeld, C.W.; Chorkendorff, I. Adsorption of hydrogen on clean and modified magnesium films. *Phys. Rev. B* **2006**, *74*, 193408:1–193408:4.
83. Cheung, S.; Deng, W.-Q.; van Duin, A.C.T.; Goddard, W.A., III. ReaxFFMgH reactive force field for magnesium hydride systems. *J. Phys. Chem. A* **2005**, *109*, 851–859.
84. Du, A.J.; Smith, S.C.; Yao, X.D.; Lu, G.Q. *Ab initio* studies of hydrogen desorption from low index magnesium hydride surface. *Surf. Sci.* **2006**, *600*, 1854–1859.

85. Du, A.J.; Smith, S.C.; Lu, G.Q. First-principle studies of the formation and diffusion of hydrogen vacancies in magnesium hydride. *J. Phys. Chem. C* **2007**, *111*, 8360–8365.
86. Wu, G.; Zhang, J.; Li, Q.; Wu, Y.; Chou, K.; Bao, X. Dehydrogenation kinetics of magnesium hydride investigated by DFT and experiment. *Comput. Mater. Sci.* **2010**, *49*, S144–S149.
87. Park, M.S.; Janotti, A.; van de Walle, C.G. Formation and migration of charged native point defects in MgH2: First-principles calculations. *Phys. Rev. B* **2009**, *80*, 064102:1–064102:5.
88. Fernandez, J.F.; Sanchez, C.R. Rate determining step in the absorption and desorption of hydrogen by magnesium. *J. Alloys Compounds* **2002**, *340*, 189–198.
89. Huot, J.; Liang, G.; Baily, S.; van Neste, A.; Schulz, R. Structural study and hydrogen sorption kinetics of ball-milled magnesium hydride. *J. Alloys Compounds* **1999**, *293–295*, 495–500.
90. Bader, R.F.W. *Atoms in Molecules: A Quantum Theory*, 1st ed.; Oxford University Press: New York, NY, USA, 1994.
91. Novaković, N. *Ab initio* Study of Alkali, Alkali-earth, and Transition Metals Hydrides' properties, Ph.D. Thesis (in Serbian), Faculty of Physics, University of Belgrade, Belgrade, Serbia, 2010.
92. Milanović, I. A theoretical study of surface effects on desorption kinetics o hydrogen from MgH_2, Master Thesis (in Serbian), Faculty of Physical Chemistry, University of Belgrade, Belgrade, Serbia, 2011.
93. Kurko, S.; Paskaš-Mamula, B.; Matović, L.J.; Grbović Novaković, J.; Novaković, N. The influence of boron doping concentration on MgH_2 electron structure. *Acta Phys. Pol. A* **2011**, *120*, 238–241.
94. Kurko, S.; Matović, L.J.; Novaković, N.; Matović, B.; Jovanović, Z.; Paskaš-Mamula, B.; Grbović Novaković, J. Changes of hydrogen storage properties of MgH_2 induced by boron ion irradiation. *Int. J. Hydrogen Energy* **2011**, *36*, 1184–1189.
95. Kecik, D.; Aydinal, M.K. Density functional and dynamics study of the dissociative adsorption of hydrogen on Mg (0001) surface. *Surf. Sci.* **2009**, *603*, 304–310.
96. Gellat, C.D., Jr.; Ehrenreich, H.; Weis, J.A. Transition-metal hydrides: Electronic structure and the heats of formation. *Phys. Rev. B* **1978**, *17*, 1940–1957.
97. Nørskov, J.K.; Besenbacher, F. Theory of hydrogen interaction with metals. *J. Less-Common Metals* **1987**, *130*, 475–490.
98. Hammer, B.; Nørskov, J.K. Electronic factors determining the reactivity of metal surfaces. *Surf. Sci.* **1995**, *343*, 211–220.
99. Harrison, W.A. *Elementary Electronic Structure*; World Scientific: Singapore, 1999; p. 539.
100. Van Essen, R.M.; Buschow, K.H.J. Hydrigen absorption in various zirconium and hafnium based intermetallic compounds. *J. Less-Common Metals* **1979**, *64*, 277–284.
101. Kadir, K.; Sakai, T.; Uehara, I. Synthesis and structure determination of a new series of hydrogen storage alloys: RMg_2Ni_9 (R = La, Ce, Pr, Nd, Sm and Gd) build from $MgNi_2$ laves-type layers alternating with AB_5 layers. *J. Alloys Compounds* **1997**, *257*, 115–121.
102. Tatsumi, K.; Tanaka, I.; Inui, H.; Tanaka, K.; Yamaguchi, M.; Adachi, H. Atomic structures and energetics of $LaNi_5$–H solid solution and hydrides. *Phys. Rev. B* **2001**, *64*, 184105:1–184105:10.
103. Riabov, A.B.; Yartys, V.A. An interrelation of RH*x* coordination and H ordering in the structures of intermetalic hydrides. *J. Alloys Compounds* **2002**, *330–332*, 234–240.

104. Soubeyroux, J.L.; Fruchart, D.; Derdour, S.; Vuillet, P.; Rouault, A. Localization of hydrogen (deuterium) in Hf_2FeD_x (x = 0–5). *J. Less-Common Metals* **1987**, *129*, 187–195.
105. Vuillet, P.; Teisseron, G.; Oddou, J.L.; Jeandey, C.; Yaouanc, A. Changes in the crystallographic and magnetic properties of Hf_2Fe on hydrogen absorption. *J. Less-Common Metals* **1984**, *104*, 13–20.
106. Ivanović, N.; Rodić, D.; Koteski, V.; Radisavljević, I.; Novaković, N.; Marjanović, D.; Manasijević, M.; Koički, S. Cluster approach to the Ti_2Ni structure type. *Acta Crystallogr. B* **2006**, *62*, 1–8.
107. Cekić, B.; Ivanović, N.; Koteski, V.; Koički, S.; Manasijević, M. The electronic structure of Hf_2Co: Perturbed angular correlation study and first principle calculations. *J. Phys. Condens. Matter* **2004**, *16*, 3015–3026.
108. Koteski, V.; Ivanović, N.; Cekić, B.; Milošević, Z. FP-LAPW study of Hf_2Ni: Structure, electronic properties and electric field gradients. *J. Phys. Soc. Jpn.* **2004**, *73*, 2158–2163.
109. Akbarzadeh, A.R.; Ozoliņš, V.; Wolverton, C. First-principles determination of multicomponent hydride phase diagrams: Application to the Li–Mg–N–H system. *Adv. Mater.* **2007**, *19*, 3233–3239.
110. Vajeeston, P.; Ravindran, P.; Kjekshus, A.; Fjellvåg, H. Theoretical modeling of hydrogen storage materials: Prediction of structure, chemical bond character, and high-pressure behaviour. *J. Alloys Compounds* **2005**, *404–406*, 377–383.
111. Ravindran, P.; Vajeeston, P.; Vidja, R.; Fjellvåg, H.; Kjekshus, A. Modeling of hydrogen storage materials by density-functional calculations. *J. Power Sources* **2006**, *159*, 88–99.
112. Kim, K.C.; Sholl, D.S. Crystal structures and thermodinamic investigation of $LiK(BH_4)_2$, KBH_4, $NaBH_4$, from first principle calculations. *J. Phys. Chem. C* **2010**, *114*, 678–686.
113. Hector, L.G., Jr.; Herbst, J.F. Density functional theory for hydrogen storage materials: successes and opportunities. *J. Phys. Condens. Matter* **2008**, *20*, 064229:1–064229:11.
114. Balogh, M.P.; Jones, C.Y.; Herbst, J.F.; Hector, L.G., Jr.; Kundrat, M. Crystal structures and phase transformation of deuterated lithium imide, Li_2ND. *J. Alloys Compounds* **2006**, *420*, 326–336.